Scientific Journal of Silesian University of Technology. Series Transport
Zeszyty Naukowe Politechniki Śląskiej. Seria Transport

Volume 129 **2025**

p-ISSN: 0209-3324

e-ISSN: 2450-1549

DOI: https://doi.org/10.20858/sjsutst.2025.129.10

Journal homepage: http://sjsutst.polsl.pl

Article citation information:
Nguyen, N.H.Q., Nguyen, N.Q.N., Nechaev, V.N. Optimizing alternative air traffic service routes for airport disruption contingency management. *Scientific Journal of Silesian University of Technology. Series Transport*. 2025, **129**, 169-190. ISSN: 0209-3324. DOI: https://doi.org/10.20858/sjsutst.2025.129.10

Ngoc Hoang Quan NGUYEN[1], Ngoc Quynh Nhu NGUYEN[2], Vladimir Nikolaevich NECHAEV[3]

OPTIMIZING ALTERNATIVE AIR TRAFFIC SERVICE ROUTES FOR AIRPORT DISRUPTION CONTINGENCY MANAGEMENT

Summary. Flight disruptions due to destination airport unavailability present significant challenges for air traffic management and airline operations. These situations may lead to cascading delays, increased fuel consumption, and reduced passenger satisfaction. A key response strategy is the timely identification of alternative air traffic services (ATS) routes to suitable diversion airports while ensuring flight safety and operational continuity. However, existing diversion approaches often rely on static contingency plans or real-time decisions by air traffic controllers, which may not perform well under dynamic conditions. To address this, a robust multi-objective optimization model based on the A-star algorithm is proposed to dynamically identify optimal alternative air traffic services routes when the planned destination becomes inaccessible. The model accounts for multiple objectives, including route efficiency, safety, and operational feasibility, across pre-tactical and tactical phases of air traffic flow management. By integrating airspace constraints and traffic flow considerations, the model supports adaptive, data-informed decision-making. Simulation results demonstrate

[1] Faculty of aviation operation, Vietnam Aviation Academy, Vietnam. Email: quannnh@vaa.edu.vn. ORCID: https://orcid.org/0009-0003-8873-9263
[2] Faculty of Information Technology, Gia Dinh University, Vietnam. Email nhunnq@giadinh.edu.vn. ORCID: https://orcid.org/ 0009-0004-0806-7477
[3] Department of Air Traffic Control, Moscow State Technical University of Civil Aviation, Russia. Email: v.nechaev@mstuca.ru. ORCID: https://orcid.org/0009-0005-9610-9397

the model's ability to reduce network disruptions and support safe, efficient diversions under various traffic scenarios. This study contributes to enhancing the resilience of the air transportation system and provides a foundation for future integration into intelligent air traffic management tools and decision support systems.

Keywords: alternative ATS route, air traffic management, destination airport unavailable, A* algorithm, multi-objective optimization model

1. INTRODUCTION

Air transportation is a cornerstone of global connectivity, but it is inherently vulnerable to disruptions caused by adverse weather, technical malfunctions, security threats, and other unforeseeable events. In the event of airport inoperability, aircraft must be promptly reassigned to alternative destinations through optimized ATS routing to ensure safety, reduce economic impact, and sustain operational continuity

Recent statistical data underscores the significance of this issue. According to the U.S. Bureau of Transportation Statistics (BTS, 2025), a total of 15,059 flights operated by the ten major airlines were diverted to alternate airports in 2024 alone, compared to 14,864 in 2023. Similarly, data from Eurocontrol (2024) reveals that in 2022, out of 9.3 million flights within the EUROCONTROL Network Manager area, 28,738 flights (0.3%) landed at an airport different from their originally intended destination, and the estimated cost per diverted flight was approximately €8,800. In addition to direct operational costs, unplanned diversions impose significant financial burdens on airlines, airports, and passengers. According to the Federal Aviation Administration (FAA, 2020), the variable operating cost per flight hour is $1,508, while the average cost of a flight cancellation per passenger is approximately $15.51. These figures, when multiplied across thousands of diverted flights annually, represent substantial economic losses for the aviation industry. Beyond monetary considerations, flight diversions also contribute to logistical challenges, including increased air traffic congestion, additional fuel consumption, crew scheduling complexities, and passenger inconvenience. Moreover, flight diversions cause ripple effects beyond immediate disruptions. They can delay connecting flights, burden ATC and alternate airports, and strain limited resources. Prolonged ground delays and passenger reallocation may also damage airline reputation and customer loyalty, with lasting impacts on passenger behavior.

Although diverted flights account for a small portion of total operations, their cumulative impact on ATM efficiency and safety is significant. This underscores the need for advanced strategies to identify alternative ATS routes, supported by real-time adaptive ATM systems and predictive analytics. Emerging approaches increasingly rely on optimization models powered by AI and advanced algorithms, enabling real-time disruption prediction and route optimization. However, despite their promise, the application of such innovations to the dynamic selection of alternative ATS routes remains an underexplored area. Most existing studies tend to address peripheral topics rather than directly confronting this critical challenge.

Several notable studies have explored optimization techniques relevant to trajectory adjustments. Xu et al. (2020) proposed a collaborative ATFM framework utilizing Mixed-Integer Linear Programming to optimize cost-efficient trajectory adjustments and minimize delays for airspace users. Similarly, Yang et al. (2021) introduced a robust optimization model designed to enhance adaptability and efficiency in identifying alternative ATS routes for flights under uncertain adverse weather conditions. Another study focused on a robust optimization framework for flight diversions under uncertainty, balancing stakeholder interests with operational performance (Bongo and Sy, 2020). However, the aforementioned studies primarily focus on optimizing real-time or pre-tactical trajectory adjustments for aircraft, rather than developing a comprehensive optimization framework capable of determining alternative routes when the original ATS route becomes unavailable. More notably, there is a near absence of research dedicated to identifying alternative routes when the original destination airport (or transfer of control point) is rendered unusable. This gap highlights a promising research direction focused on developing an advanced optimization model that can dynamically identify alternative ATS routes across different phases of ATFM (pre-tactical, or tactical), while satisfying specific operational constraints and performance objectives.

In light of these challenges, it is essential to develop an optimized decision-support framework for identifying alternative ATS routes when the planned destination airport becomes unavailable. This study proposes a robust model based on the A* algorithm to determine the most efficient route to an alternate airport under two cases. The first involves the unavailability of the destination airport alone – due to technical issues or on-ground incidents – while the second addresses broader disruptions, including surrounding airspace and portions of the original route (hereafter referred to as the No-fly Area), as seen in adverse weather or airspace restrictions. These cases present varying levels of complexity, particularly in maintaining regulatory compliance and safety. In both cases, the model aims to minimize total flight distance to ensure operational efficiency and feasibility.

To address the added complexity of the second case, three routing scenarios with additional sub-objectives are introduced: (1) minimizing deviation from the original route, (2) minimizing the total distance from the original start to the new destination, and (3) enabling user-defined preferences for flexible routing. These scenarios enhance the model's practical applicability across different ATFM phases. Scenarios 1 and 2 are best suited for pre-tactical planning, where minimizing flight time (Scenario 2) or maintaining route consistency (Scenario 1) supports efficiency and conflict avoidance. Scenario 3, offering flexible user input, is more appropriate for the tactical phase, which requires real-time responsiveness to actual traffic and airspace conditions.

To evaluate the efficiency and responsiveness of the proposed model in dynamically identifying alternative ATS routes, the ATS route network within the HCM FIR has been selected as the primary case study. The HCM FIR holds a strategically significant geographical position (Carreras and Greenman, 2017; Nguyen Le Quyen, 2022), serving as a critical aviation hub that connects countries in the Northern Hemisphere – particularly Russia and China – to those in the Southern Hemisphere, including Oceania. Additionally, it borders the vast South China Sea, a region that accommodates multiple crucial international ATS routes. In addition to its strategic location, Vietnam has one of the fastest-growing aviation industries in the world (International Trade Administration, 2024; 6Wresearch, 2022). The country's air transport sector has experienced significant expansion in recent years, driven by increasing passenger demand, economic growth, and enhanced connectivity with global markets. The HCM FIR plays an essential role in facilitating this growth, serving as a critical gateway for both domestic and international air traffic. Another key factor that underscores its significance is the relatively high air traffic density on several routes within the FIR. For instance, the HCM – Hanoi route, which largely falls within this FIR, ranks as the fourth busiest domestic air route in the world (OAG, 2024). Furthermore, the weather conditions in this region can be highly complex at times due to the influence of monsoons and tropical storms originating from the South China Sea. These adverse weather patterns frequently disrupt flight schedules, requiring not only frequent ATS route reconfigurations but also necessitating aircraft diversions to alternate airports.

A notable example occurred on May 16, 2023, when seven flights originally scheduled to land at Tan Son Nhat International Airport were unable to do so and had to divert to alternate airports due to unfavorable weather conditions (Vietnamplus, 2023). Given these factors, selecting the HCM FIR as a case study is highly appropriate, as it ensures both practical relevance and a robust scientific foundation. Moreover, the insights gained from this analysis can enhance the potential for broader implementation in other high-density airspaces worldwide, particularly in regions where adverse weather conditions frequently necessitate the identification of alternative ATS routes and airport diversions.

2. METHODOLOGY FOR OPTIMIZING ALTERNATIVE ATS ROUTES DURING AIRPORT DIVERSIONS

2.1. A* algorithm

The A* algorithm is one of the most widely used and efficient pathfinding algorithms in computer science and artificial intelligence. It is a heuristic search algorithm that extends Dijkstra's Algorithm by incorporating heuristic information to improve efficiency (Beeker, 2004). The fundamental principle of A* is to find the shortest route between a start node and a goal node in a weighted graph while balancing exploration and optimality. A* operates using a cost function:

$$f(n) = g(n) + h(n) \tag{1}$$

where:
g(n) represents the actual cost from the start node to node n,
h(n) is the heuristic estimate of the cost from n to the goal,
f(n) is the estimated total cost of the path through node n.

The choice of heuristic function significantly influences the performance of A*, with an admissible (never overestimates the true cost) and consistent (follows the triangle inequality) heuristic ensuring both optimality and efficiency. Compared to uninformed search methods, A* intelligently prioritizes promising paths, reducing unnecessary exploration and enhancing computational speed. It guarantees an optimal solution if the heuristic function does not overestimate the actual cost. This characteristic makes A* particularly effective in solving shortest route problems in large-scale environments. The algorithm's ability to balance accuracy and efficiency has made it a fundamental tool in artificial intelligence and operations research. Its scalability and robustness ensure its continued relevance in modern computational problem-solving, making it one of the most powerful techniques for optimal pathfinding in complex systems, including transportation networks (Felix et al, 2024; Wang et al., 2024), robotic navigation (Ju et al, 2020; Kabir et al, 2024), and game environments (Kurniawan et al, 2024), where real-time decision-making and adaptability are crucial for efficiency and performance.

In the field of aviation in general and ATM in particular, the A* algorithm has been widely applied to determine optimal flight routes for both manned civil aircraft (Ma et al. 2022; Neretin et al. 2021; Li et al. 2023; Roy, 2023) and unmanned aerial vehicles (Mandloi et al. 2021; Ji et al. 2024). However, most existing studies focus on initial trajectory planning rather than the dynamic re-routing of ATS paths under operational constraints. This research addresses that gap by proposing a re-routing model capable of optimizing alternative ATS routes while ensuring efficiency and regulatory compliance. Designed for use across pre-tactical and tactical phases, the model adapts to diverse scenarios and disruptions, enhancing the flexibility and resilience of ATS route planning in complex airspace environments.

2.2. Steps for Developing Optimization Models and Mathematical Models

Since the A-Star (A*) algorithm is a branch of graph theory, the airspace structure in this study is represented as a graph $G = (N,O)$ where $N = \{N_0, N_1, N_2, \ldots, N_l\}$, and $O = \{O_1, O_2, \ldots, O_k\}$. In this representation, N consists of waypoints and airport coordinates (collectively referred to as nodes), while O represents the arcs, each defined as a direct connection between two nodes. Each arc O is characterized by two key parameters: distance (d) and angle (θ).

A crucial aspect of data preprocessing is ensuring the accurate input of node coordinates, as precise spatial representation is fundamental for effective route optimization. To achieve this, the latest aeronautical data from the Vietnam AIP 2024 is utilized, incorporating a total of 130 nodes into the airspace model. Figure 1 illustrates the spatial relationships among these nodes, providing a graphical representation of the airspace network structure.

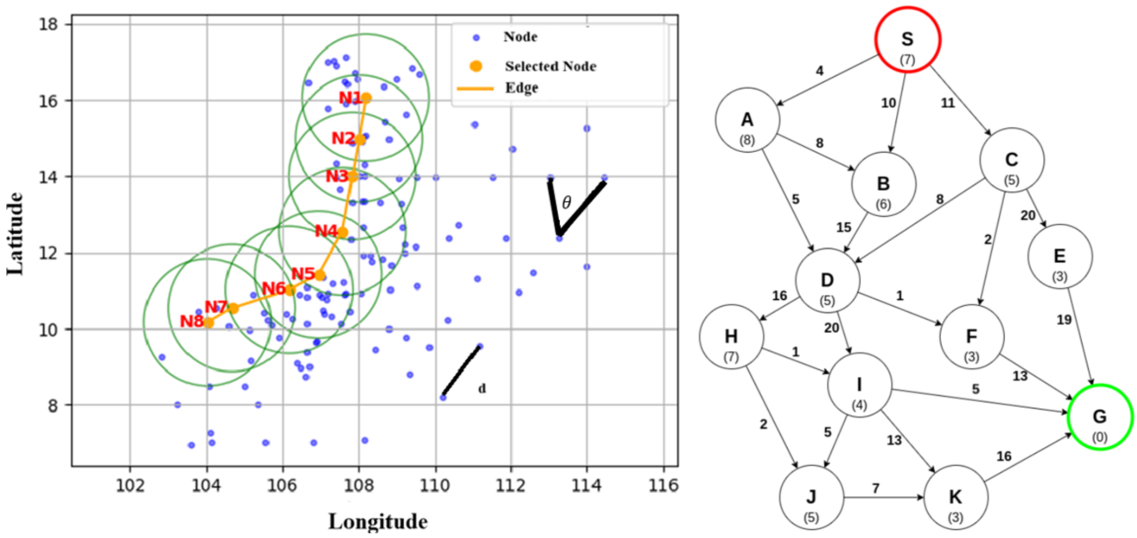

Fig. 1. Illustrating the Structure of Airspace in the Model
and Establishing Relationships Between Nodes

After completing the airspace structure description using nodes, the next step is to establish relationships between them, specifically defining parent-child connections. This hierarchical relationship is essential for optimizing route search processes. Given that the HCM FIR encompasses both land and sea areas, the airspace structure is systematically divided into two distinct regions: land–coast and coast-sea. To determine how nodes are connected, a systematic selection process is applied. Each node identifies neighboring nodes within a specified radius, forming a structured network. The node at the center of this defined area is designated as the parent node, while all surrounding nodes that fall within the radius are considered child nodes. A directional scanning technique is used, where the search is conducted in one-degree increments. In each direction, at most one child node is selected, ensuring an even distribution of connections and preventing unnecessary redundancy. This method enhances the efficiency of route calculations and ensures a well-structured node hierarchy for optimal airspace navigation. Figures 2 and 3 illustrate all node connections in the land – coast and coast – sea regions, respectively. Land nodes are shown in green, sea nodes in blue, and coastal nodes – appearing in both figures – are marked in pink.

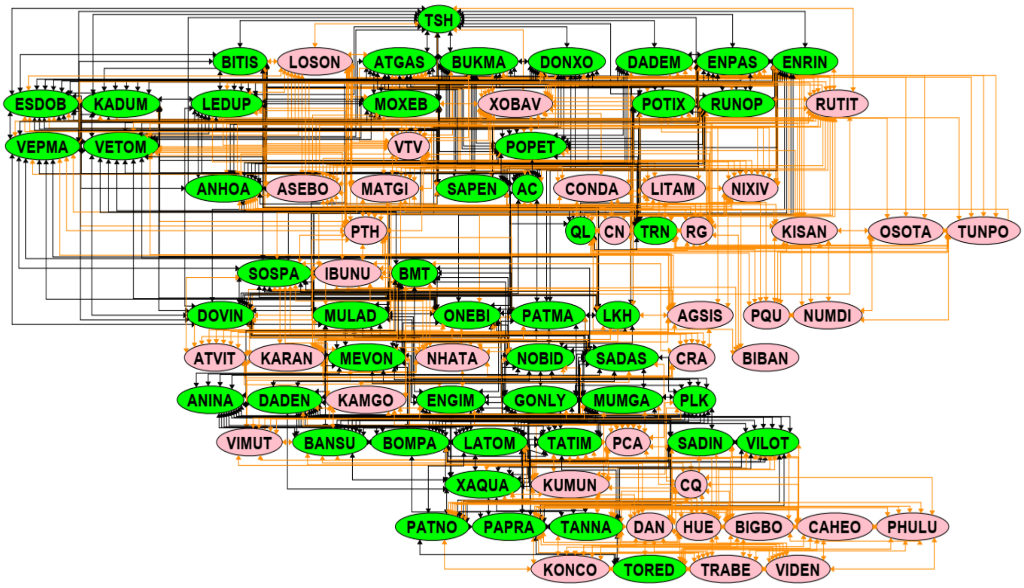

Fig. 2. Connections between all nodes in the land-coast region

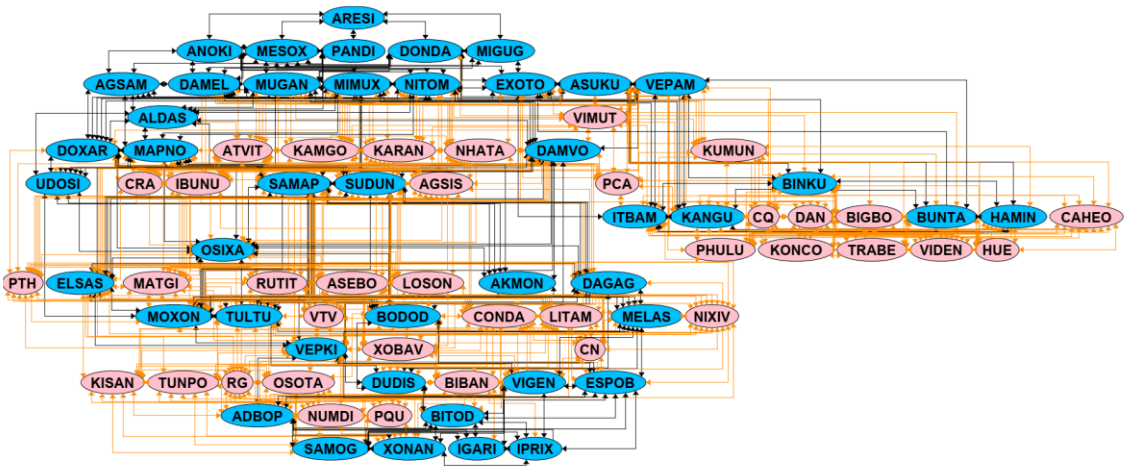

Fig. 3. Connections between all nodes in the coast-sea region

The next crucial step in the model development is the precise definition of the objective function, constraints, and assumptions that will be applied within the model. This phase is fundamental, as it forms the conceptual and mathematical backbone of the model, ensuring its effectiveness, feasibility, and real-world applicability. Without a well-defined structure, even the most sophisticated models may fail to produce meaningful or actionable insights. In this model, the primary objective, across all scenarios and cases, is to minimize the distance of the alternative route to the newly designated airport, as specified by the user. This objective is particularly important in urban planning, logistics, and transportation network optimization, where shorter travel distances directly translate to lower operational costs, reduced travel time, and improved user satisfaction. The objective function is defined mathematically as:

$$D = \min \sum_{i=0}^{u-1} d_{i,i+1} \tag{2}$$

where:
d is the distance between any two consecutive nodes i and $i+1$ on the ATS route that consists of u nodes.
D is the total distance from the starting node to the ending node.

For each ATS route, the following variables are defined:

- P_i^a: A node positioned along ATS route a between the start and end node, defined by its latitude and longitude. Note: $i \in N_n$, indicating that for each ATS route a, the node i ranges from 0 to n. Specifically:
  When $i = 0$, it corresponds to the starting node of ATS route a and must coincide with the starting point of the original route.
  When $i = n$, it corresponds to the ending node of ATS route a and must not coincide with the ending point of the original ATS route. In other words, n represents the newly selected destination airport.
- (x_i, y_i): Indicates the latitude and longitude of the node i.
- $d_{i,i+1}^a$: The length of the arc connecting node i to node $i+1$ along ATS route a.

  This value is calculated using the following formula.

$$d_{i,i+1}^n = \sqrt{(x_i - x_{i+1})^2 + (y_i - y_{i+1})^2} \tag{3}$$

- $O_{i,j}^a$: The arc i to j on ATS route a.

The variable $O_{i,j}^a$ is defined as a binary variable, specifically:

$$O_{i,j}^a = \begin{cases} 1, & \text{if the arc from } i \text{ to } j \text{ belongs to ATS route } a; \\ 0, & \text{other cases.} \end{cases} \tag{4}$$

Some special variables related to the original ATS route t are listed as follows:

- P_0^t: represents the starting node on the ATS route t.
- P_i^t: represents the node at position i on the ATS route t.
- P_m^t: represents the ending node on the ATS route t that cannot be used.
- Q_q^t: The area q of a polygonal area containing the original destination airport of route t within the structured airspace $G = (N, O)$, where aircraft operations are limited.
- R_r^t: A circle with radius r centered at a designated point, contains the original destination airport of route t within the structured airspace $G = (N, O)$, where aircraft operations are limited.

In this study, when the initial ATS route t encounters a No_fly_area in the form of a circular with radius R_r^t or a polygonal area Q_q^t, an alternative ATS route a must be identified to avoid these limited area and reach a newly designated airport specified by the user (when at least one No_fly_area contains the original destination airport). In cases where only the node P_m^t representing the destination airport is limited, the aircraft will be unable to use this location.

- Node: $\forall\ P_i^t \in$ N, (P_i^t, v) $\notin$ O: In a blocked state, P_i^t cannot establish any arcs to any other node, where v is any node belonging to *N*. In this case:

$$\begin{cases} \forall P_i^a \neq P_m^t \\ P_i^t = \varnothing \end{cases} \tag{5}$$

– Circular area:

$$\sum\sqrt{(x_i - x_r)^2 + (y_i - y_r)^2} \geq R_r^t, \forall i \in N_n \text{ and } O_{n-1,n}^a \cap R_r^t = \varnothing \tag{6}$$

– Polygon area:

$$\sum O_{i,j}^a \cap Q_q^t = 0,\ \forall O_{i,j}^a \in O_n \text{ and } O_{n-1,n}^a \cap Q_q^t = \varnothing \tag{7}$$

In Case 1 and Scenario 2 of Case 2, when determining an alternative route for the original route due to a change in the destination airport, and this airport is limited either as a single point, within a polygonal region, or within a circular area, compliance with Equation (2) and one of the Equations (5), (6), or (7), corresponding to the shape of the No_fly_area, must be ensured. Additionally, the following equation must also be satisfied.

$$\begin{cases} P_0^a \equiv P_0^t \\ P_n^a \neq P_m^t \\ \exists O_{k,n}^a = 1 \end{cases} \tag{8}$$

For Scenario 1 in Case 2, in addition to satisfying Equation (2) and one of the three Equations (5), (6), or (7) depending on the shape of the No_fly_area, an additional objective function will be formulated. This function aims to ensure that the alternative route changes as little as possible from the original route while still avoiding all No_fly_area that the original route intersected, including at least one area containing the original destination airport.

$$\begin{cases} O_{i,j}^a \cap (R_r^t \cup Q_q^t) = \varnothing \\ \min \sum\limits_{(i,j)\in O} \left| O_{i,j}^a - O_{i,j}^t \right| \\ \exists h \in N \text{ such that } O_{i,h} \text{ is the first arc that deviates from } t \text{ and is non-collinear with } t \\ \exists l \in N \text{ such that } O_{l,j} \text{ is the last arc before returning to } t \text{ and is non-collinear with } t \end{cases} \tag{9}$$

In Scenario 3, to ensure flexibility, users are given the option to reutilize nodes from the original route *t*, excluding those located within any designated No_fly_area, to construct an alternative route *a*. An additional objective function will be built:

$$
\begin{cases}
\forall P_i^a \in N_m, O_{i,j}^a \cap (R_r^m \cup Q_q^m) = \varnothing \\
\sum_x O_{x,i}^a = 1,\ \sum_z O_{j,z}^a = 1,\ \mathrm{x} \in \mathrm{N}, \mathrm{z} \in \mathrm{N} \\
\exists h \in N, \text{ with } h < j \text{ such that } O_{i,h}^n \text{ is a non-collinear segment with } m, \text{ or} \\
\exists l \in N, \text{ with } l > i \text{ such that } O_{l,j}^n \text{ is a non-collinear segment with } m
\end{cases}
\tag{10}
$$

In equations (9) and (10), i represents the last available node before all No_fly_area, and j represents the first available node after all No_fly_area along the route t.

Once the objective functions are established, the model's fundamental constraints will be identified and mathematically expressed as equations.

Constraint 1: An ATS route a must establish a continuous path between the start node and the end node, ensuring that no arcs lead into the start node or originate from the end node. This constraint is mathematically represented by two equations.

$$
\sum_{j \in N^{a^+}(N_0^a)} O_{N_0^a,j}^a - \sum_{j \in N^{a^-}(N_0^a)} O_{j,N_0^a}^a = 1,\ \forall a \tag{11}
$$

$$
\sum_{j \in N^{a^-}(N_n^a)} O_{j,N_n^a}^a - \sum_{j \in N^{a^+}(N_n^a)} O_{N_n^a,j}^a = 1,\ \forall a \tag{12}
$$

Constraint 2: For each intermediate node i (excluding the start and end nodes), the number of incoming arcs must equal the number of outgoing arcs. This flow balance condition is represented by Equation (13).

$$
\sum_{i \in N^-(j)} O_{i,j}^a = \sum_{i \in N^+(j)} O_{j,i}^a,\ \ \forall j \in N_a - \{0, n\} \tag{13}
$$

To ensure that the model can function effectively across all phases of ATFM while maintaining both operational feasibility and alignment with real-world conditions, a set of well-defined assumptions is established. These assumptions aim to balance the model's practical applicability with its optimization objectives, ensuring that real-world constraints are incorporated without significantly compromising computational efficiency or solution quality. By defining these operational conditions in advance, the model can better accommodate the complexities of ATM while maintaining robustness and adaptability to dynamic cases:

- Navigation Infrastructure: All navigation systems, including Non-Directional Beacons, VHF Omnidirectional Range, and Global Navigation Satellite Systems, are assumed to function reliably, providing continuous and consistent coverage within designated areas. In the event of system failures, relevant notifications will be issued, and affected nodes will be removed from the input graph to maintain model integrity.
- Airspace Organization and Utilization: The structure and boundaries of controlled airspace are considered static and unchanging throughout the operational period. During pre-tactical phases, any establishment of a No_fly_area due to military operations or other restricted activities will be communicated in advance to ATFM units to facilitate appropriate planning and adjustments.
- Meteorological Conditions: Adverse weather phenomena are assumed to be forecasted accurately, allowing them to be represented as polygons or circular areas defined by precise

coordinates for integration into the model. This ensures that weather constraints are effectively incorporated into operational planning.
- Aircraft Operations: All aircraft are assumed to operate under standard protocols without disruptions or priority handling due to emergencies or unforeseen contingencies.
- The model assumes that all nodes are accessible for the selection of alternative ATS routes, except those explicitly restricted by predefined constraints. The connections between these nodes are established based on geographic proximity and operational viability, ensuring that all generated routes conform to existing airspace structures.

To ensure the flexibility, dynamism, and adaptability of the model, No_fly_area will be dynamically defined by inputting coordinate data based on notifications received either during the planning phase or in real-time. Once these zones are established, the model will identify valid nodes and permissible connections to be incorporated into the optimization framework. This approach guarantees that alternative routes are continuously updated in alignment with real-world conditions while adhering to the existing airspace structure. Additionally, by continuously adapting to evolving constraints, the system not only optimizes operational efficiency but also upholds strict compliance with safety and regulatory frameworks.

The model's dynamic approach allows for the continuous optimization of alternative routes, taking into account real-time airspace conditions, regulatory constraints, and overall operational efficiency. By doing so, it ensures that the designated alternative route is not only precise but also practical and adaptable to evolving scenarios. This capability enhances the effectiveness of ATM and route planning by minimizing disruptions, improving flight safety, enhancing route reliability, and ensuring seamless integration with existing airspace structures, ultimately contributing to a more resilient and efficient aviation system. The final step of the model is to determine the heuristic function used. In the A-star algorithm, selecting an appropriate heuristic function is crucial, as it significantly impacts the optimization performance of the model. This has been well-documented in previous research (Foead et al., 2025; Sathvik & Patil, 2021). The authors conducted a comprehensive evaluation, and the results indicate that both the Euclidean and Gaussian heuristic functions yield optimal outcomes (Nguyen et al., 2025). However, the Euclidean function is simpler to implement. Therefore, in this model, the Euclidean heuristic function will be adopted to enhance computational efficiency while maintaining optimal performance.

3. RESULTS AND DISCUSSION

To run the model effectively, the first essential step is to identify the No_fly_area. A thorough assessment of airspace usage, particularly for military operations, was conducted, and reports from the Civil Aviation Authority of Vietnam regarding airports that frequently experience flight diversions were reviewed. Based on these analyses, several representative No_fly_areas were identified for implementation in the model, and the results are presented in this study. Regarding meteorological conditions, the complexity and variability of weather patterns make it challenging to predefine specific areas for case studies within the model. However, this limitation can be easily addressed in practical applications, as the model is designed to automatically integrate the No_fly_area data by allowing real-time data input. As a result, when deployed in real-world scenarios, the identification of restricted areas due to adverse weather conditions becomes a seamless and efficient process.

First, the results for Case 1 are presented, in which the originally designated arrival airport is unavailable for operations, while the surrounding airspace remains functional. In this scenario, it is assumed that Phu Quoc International Airport (PQU) must temporarily close due to technical equipment failure or an aircraft incident. Consequently, Can Tho International Airport (TRN) is designated as the alternate airport. The following two results will be presented: The first result examines the situation where only PQU is unavailable, affecting the establishment of ATS routes. The second result extends the analysis by considering an additional operational issue. It assumes that, in addition to PQU, the waypoints TATIM, and DONXO also become unusable due to further constraints. Figure 4 illustrates the model's results regarding the impact on initial routes across the entire ATS network due to operational disruptions at PQU, as well as the process of inputting data for the newly designated destination airport (referred to as new_end_node in our model). Table 1 presents the route analysis results, including a list of waypoints and the length of each route in the outcomes of Case 1. The analysis indicates that two affected routes must be redirected via alternative ATS routes to TRN. Figure 5 presents the results when only PQU is unavailable, while Figure 6 depicts the case where PQU, TATIM, and DONXO are all inaccessible.

```
List 1. Routes with affected end nodes:
1. Route from CRA to PQU
   Full route: CRA - SOSPA - LKH - KADUM - SAPEN - KISAN - PQU
   Affected nodes: PQU
2. Route from DAN to PQU
   Full route: DAN - TATIM - DADEN - MULAD - DONXO - POPET - KISAN - PQU
   Affected nodes: PQU
```

```
Processing route from CRA
Original end node is blocked. Please enter a new end node:
New end node: TRN

Processing route from DAN
Original end node is blocked. Please enter a new end node:
New end node: TRN
```

Fig. 4. The route analysis results are affected by Case 1

Tab. 1

The detailed results of the routes include a list of waypoints and lengths in Case 1

	Original route	Alternative route Case 1, Result 1	Alternative route Case 1, Result 2
CRA – PQU	602.243 km CRA - SOSPA - LKH - KADUM - SAPEN - KISAN - PQU	644.77 km CRA - SOSPA - LKH - KADUM - SAPEN - KISAN - TRN	644.77 km CRA - SOSPA - LKH - KADUM - SAPEN - KISAN - TRN
DAN – PQU	885.749 km DAN - TATIM - DADEN - MULAD - DONXO - POPET - KISAN - PQU	928.28 km DAN - TATIM - DADEN - MULAD - DONXO - POPET - KISAN -TRN	941.42 km DAN - LATOM - DADEN - MULAD - KADUM - POPET - KISAN - TRN

Based on the results from Figures 5, 6, and Table 1, it is evident that the model operates accurately when identifying a new route to the newly designated destination airport, which can be easily adjusted according to user needs. This adaptability ensures that users can flexibly modify the destination based on their specific needs without compromising the integrity of the routing process. The model dynamically adjusts the path while maintaining computational efficiency and consistency, making it highly suitable for real-world applications. For the CRA - PQU route, the results from both runs of the model are identical because the two waypoints, TATIM and DONXO, in the second result do not belong to the original route. Consequently, their presence does not interfere with the route calculation process, and the new path to the airport remains unchanged. This highlights the robustness of the model in preserving optimal paths when external constraints do not affect the original route structure. However, for the DAN - PQU route, both TATIM and DONXO are integral parts of the original route. As a result, in the second scenario, the alternative route must also avoid these two waypoints, leading to an increase in the total travel distance. This demonstrates the impact of waypoint constraints on the selection of alternative ATS routes and highlights the model's ability to navigate complex restrictions to generate feasible and compliant alternative ATS routes. The trade-off between distance and constraint adherence is evident in this case, reinforcing the importance of considering waypoint dependencies in routing optimization.

Next, the results of the three scenarios for Case 2 are analyzed, considering two distinct situations. Each situation involves two different No_fly_area. In the first situation, two No_fly_area are defined as polygons with the following: (14.880556, 108.0197222), (14.479444, 107.8436111), (14.333333, 107.4000000), (13.983333, 107.4166667), (13.957222, 109.0427778), (13.962500, 109.5213889), (14.771389, 108.8075000) and (10.445278, 103.7763889), (10.895556, 105.2280556), (9.959444, 105.1330556), (8.500000, 104.0833333), (9.245000, 102.8383333). Upon their integration, the model identifies affected ATS routes whose destination airports fall within these restricted zones. Notably, DAN–PQU is impacted by both No-fly Areas, while CRA–PQU is affected by one. As a result, rerouting to an alternate airport – assumed to be Côn Sơn (CN) – is required. In Scenario 3, users may choose any point outside the No-fly Area along the original route as the start_point for diversion. Table 2 provides a comparative analysis of waypoint sequences and route lengths, followed by Figures 7-10, which depict the corresponding adjusted routes and waypoints.

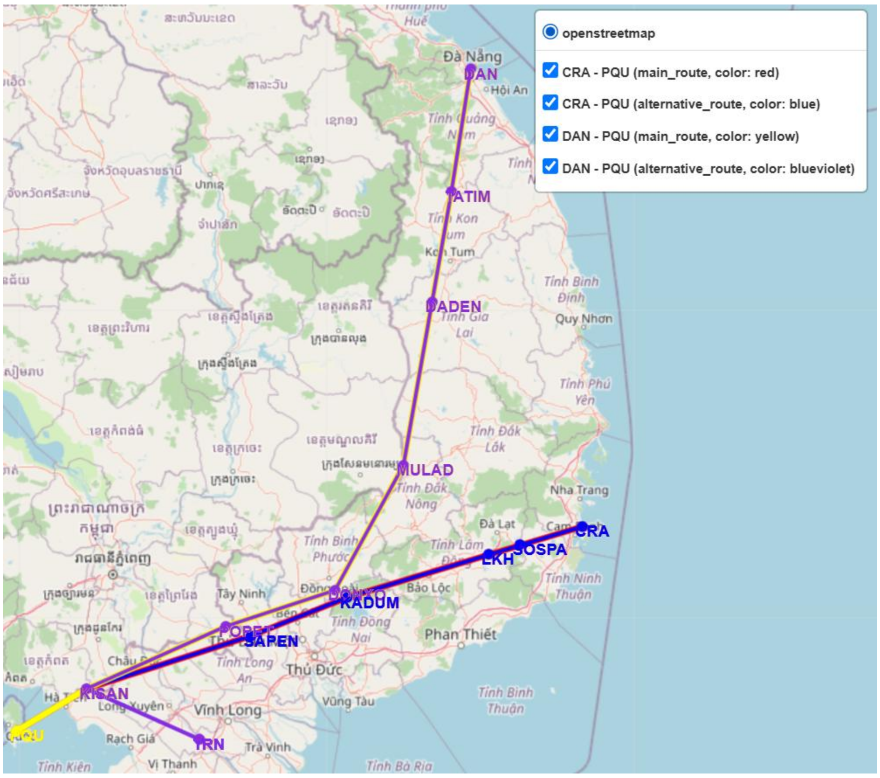

Fig. 5. Original and alternative Route configurations when PQU becomes unavailable

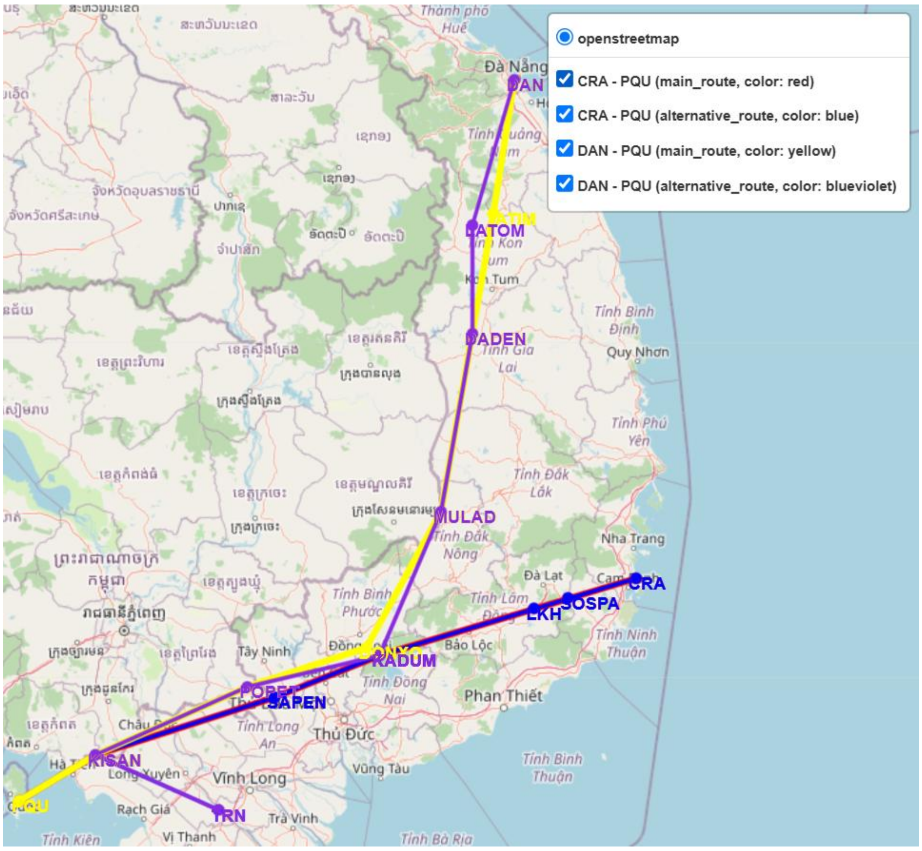

Fig. 6. Original and alternative Route configurations when PQU, TATIM, and DONXO becomes unavailable

Tab. 2

The detailed results of the routes include a list of waypoints and lengths in Situation 1, Case 2

	Original route	Alternative route – Scenario 1	Alternative route – Scenario 2	Alternative route – Scenario 3
CRA – PQU	602.243 km CRA - SOSPA - LKH - KADUM - SAPEN - KISAN - PQU	607.569 km CRA - SOSPA - LKH - KADUM - SAPEN - BITIS - CN	461.276 km CRA - ELSAS - CN	484.146 km CRA - SOSPA - LKH - RUTIT - ELSAS – CN
DAN – PQU	885.749 km DAN - TATIM - DADEN - MULAD - DONXO - POPET - KISAN - PQU	1216.229 km DAN - TATIM - KUMUN - VEPAM - KAMGO - BMT - MULAD - DONXO - POPET - BITIS - CN	989.815 km DAN - VEPAM - KARAN - ELSAS - CN	1130.605 km DAN - TATIM - KUMUN - VEPAM - KAMGO - BMT - MULAD - DONXO - ESDOB - NIXIV – CN

```
Routes with affected end nodes:
1. Route from CRA to PQU
   Full route: CRA - SOSPA - LKH - KADUM - SAPEN - KISAN - PQU
   Affected nodes: PQU
2. Route from DAN to PQU
   Full route: DAN - TATIM - DADEN - MULAD - DONXO - POPET - KISAN - PQU
   Affected nodes: PQU

Enter new end node for route 1 (from CRA to PQU): CN
Enter new end node for route 2 (from DAN to PQU): CN
```

Fig. 7. The route analysis results are influenced by Situation 1 of Case 2
and the newly input destination airport data

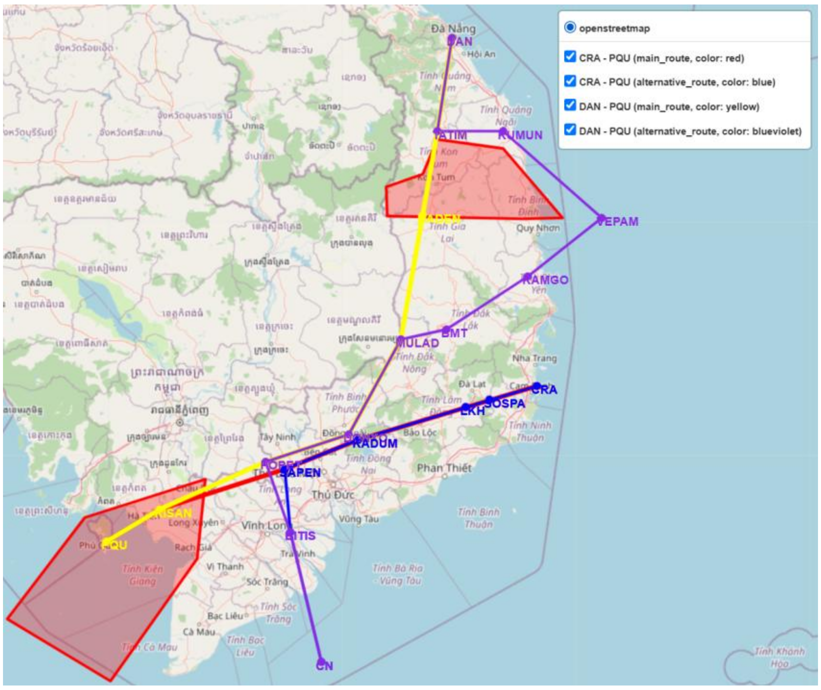

Fig. 8: Graphical results representing the routes of Scenario 1, Situation 1, Case 2

In the second situation, two No_fly_area were established: one defined as a polygon with coordinates (16.2214, 107.6013), (16.45264, 108.89553), (15.97414, 108.7921), and (15.6712, 107.8745), and another as a circular area centered at (16.052778, 108.1983333) with a radius of 50 km. Notably, these two restricted areas have overlapping regions. Following a similar approach as in the first situation, the route assessment revealed that two routes, TSH-DAN and CRA-DAN, were initially affected by the presence of these areas. As a result, an alternative ATS route was required, with Chu Lai Airport (CQ) designated as the new destination. In Scenario 3, the waypoints DADEN (TSH-DAN route) and KUMUN (CRA-DAN route) were identified as key reference points for selecting alternative ATS routes. Table 3 presents a comparative analysis of alternative routing solutions, including waypoint sequences and route lengths, while Figures 11-14 illustrate the route analysis results, new airport selection, Scenario 3 starting point, and the adjusted route visualization.

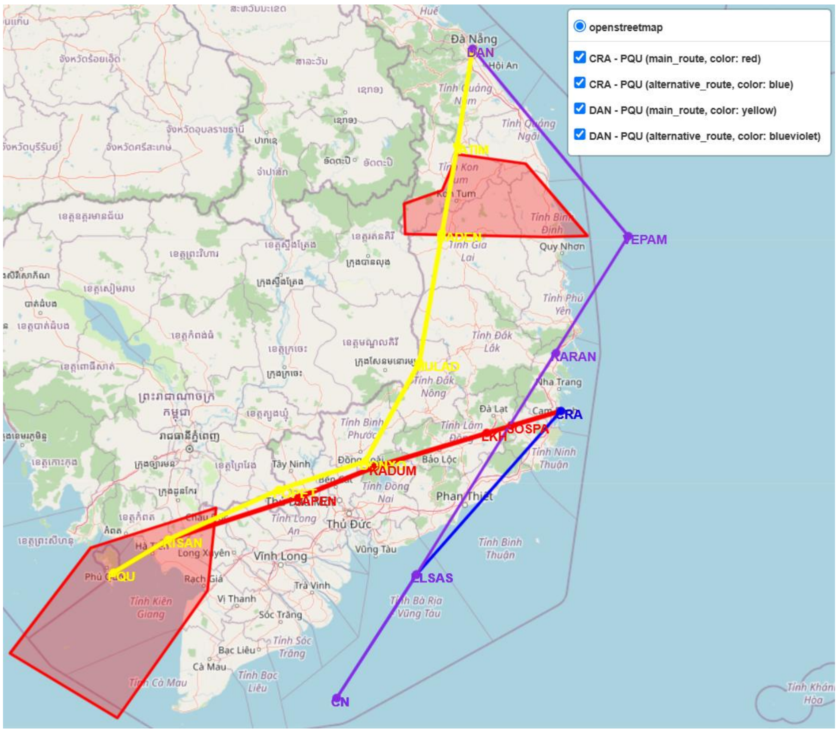

Fig. 9. Graphical results representing the routes of Scenario 2, Situation 1, Case 2

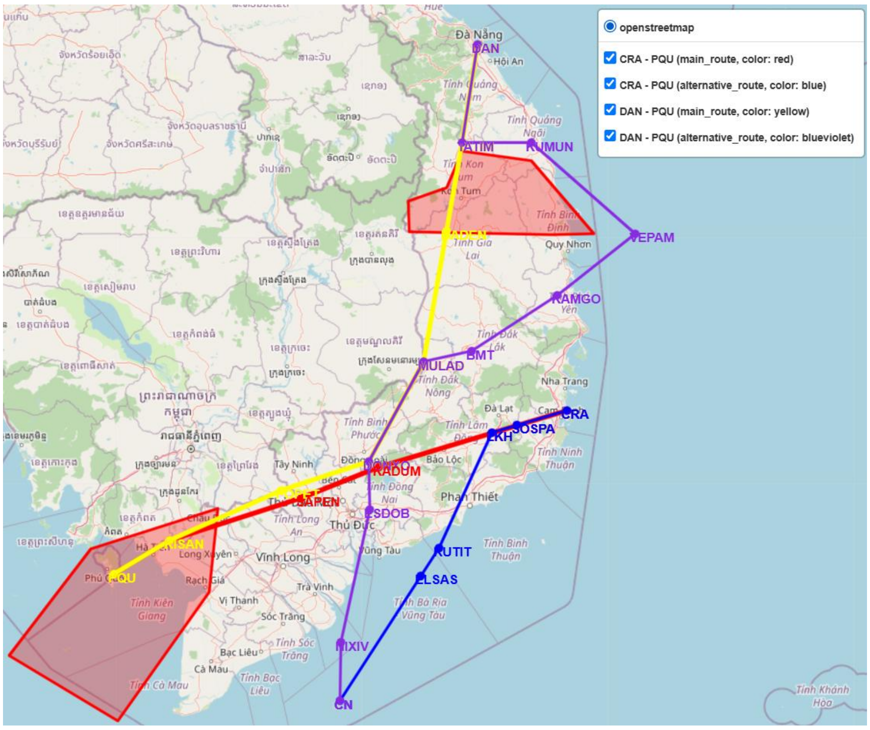

Fig. 10. Graphical results representing the routes of Scenario 3, Situation 1, Case 2

Tab. 3

The detailed results of the routes include a list of waypoints and lengths in Situation 2, Case 2

	Original route	Alternative route – Scenario 1	Alternative route – Scenario 2	Alternative route – Scenario 3
TSH – DAN	612.169 km TSH - DONXO - MULAD - DADEN - TATIM - DAN	579.203 km TSH - DONXO - MULAD - DADEN - TATIM - VILOT - SADIN - CQ	557.747 km TSH - DONXO - MULAD - MUMGA - CQ	565.615 km TSH - DONXO - MULAD - DADEN - BANSU – CQ
CRA – DAN	471.176 km CRA - KARAN - KAMGO - PCA - KUMUN - DAN	384.668 km CRA - KARAN - KAMGO - PCA - KUMUN - CQ	384.668 km CRA - KARAN - KAMGO - PCA - KUMUN - CQ	384.668 km CRA - KARAN - KAMGO - PCA - KUMUN – CQ

```
Routes with affected end nodes:
1. Route from TSH to DAN
   Full route: TSH - DONXO - MULAD - DADEN - TATIM - DAN
   Affected nodes: DAN
2. Route from CRA to DAN
   Full route: CRA - KARAN - KAMGO - PCA - KUMUN - DAN
   Affected nodes: DAN

Enter new end node for route 1 (from TSH to DAN): CQ

Enter new end node for route 2 (from CRA to DAN): CQ
```

Fig. 11. The route analysis results are influenced by Situation 2 of Case 2 and the newly input destination airport data

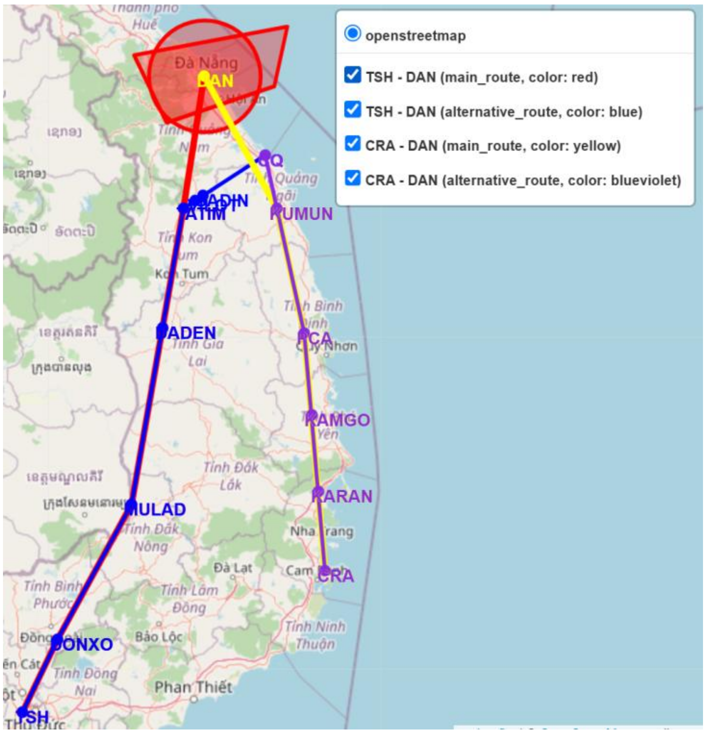

Fig. 12. Graphical results representing the routes of Scenario 1, Situation 2, Case 2

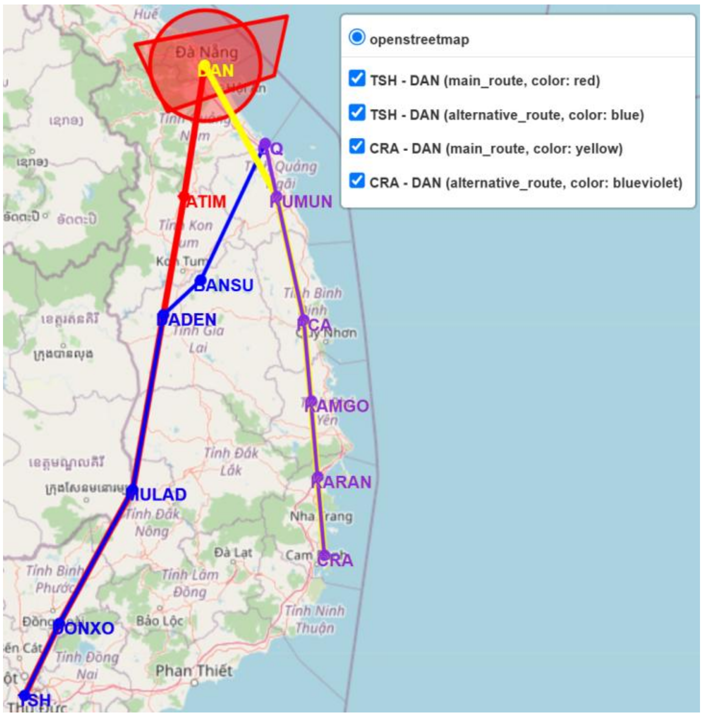

Fig. 13. Graphical results representing the routes of Scenario 2, Situation 2, Case 2

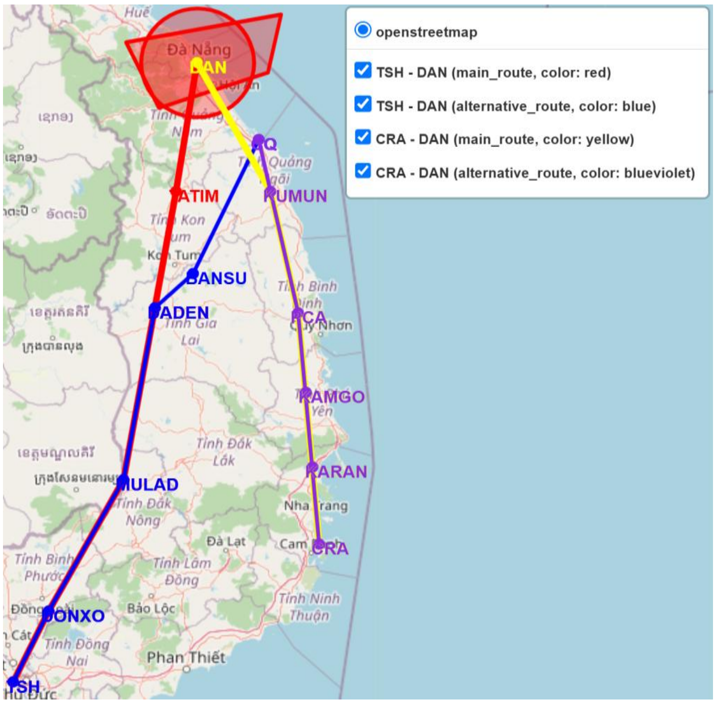

Fig. 14. Graphical results representing the routes of Scenario 3, Situation 2, Case 2

The analysis of results across all cases, including Case 1, highlights the model's remarkable flexibility and adaptability in selecting any airport as an alternative destination. Regardless of the chosen replacement airport, the model consistently generates accurate solutions that align with predefined objective functions, ensuring operational feasibility and efficiency. This adaptability is a key indicator of the model's robustness, demonstrating its capability to handle a wide range of operational constraints in dynamic ATM environments.

A more in-depth examination of the results in the two situations of Case 2 further confirms this observation. In both situations, all designed scenarios are effectively fulfilled. Specifically, in Scenario 1, the alternative ATS route closely follows the original ATS route, except for segments that require modifications to bypass the No_fly_area, as well as final adjustments necessary to reach the newly designated destination airport. In Scenario 2, the selected ATS route consistently represents the shortest among all feasible alternatives, confirming the model's ability to identify efficient alternative ATS routes. In Scenario 3, the model exhibits a high degree of flexibility by dynamically determining the alternative ATS route based on a user-specified start_point.

A particularly noteworthy observation emerged in the case of the CRA–DAN route, where the alternative ATS routes remained identical across all three scenarios. This outcome can be attributed to the fact that No_fly_area did not affect the initial segments of the original route. As a result, these segments naturally formed the shortest possible path to the destination, requiring no further optimization. This insight suggests that, in certain cases, pre-existing route structures inherently align with optimal alternative ATS route planning, thereby reducing the need for significant deviations.

Moreover, the results obtained from Situation 1 and Situation 2 collectively reinforce the model's independence from the shape, size, and distribution of the No_Fly_area. Whether these areas are separate or overlapping, the model consistently identifies the most suitable alternative ATS route while ensuring compliance with airspace regulations. This adaptability is crucial in complex airspace environments where restricted areas may change dynamically due to geopolitical constraints, military operations, or emergency airspace closures.

The simulation results indicate that the model not only successfully identifies alternative ATS routes but also ensures that these routes are operationally feasible and compatible with all phases of ATFM. This is particularly critical when one or more No_fly_area emerge due to both unforeseen circumstances, such as adverse weather conditions, security threats, or emergencies, and pre-planned situations, such as military exercises or special airspace restrictions. These disruptions can significantly impact airport operations and necessitate rapid aircraft diversions. Furthermore, the model can be applied across different ATFM phases, particularly during the pre-tactical stage, where planning and foresight are prioritized, and the tactical stage, where flexibility and real-time adaptability are crucial for responding to evolving situations. This capability is especially valuable in high-traffic airspace environments, where maintaining efficiency and safety is paramount. A key strength of the model lies in its high adaptability and ability to dynamically optimize flight routes to accommodate operational constraints. This demonstrates its practical applicability in ATM and decision-making processes, contributing to enhanced efficiency, safety, and resilience in airspace operations. In addition to enhancing the efficiency and reliability of air traffic flows, the model contributes to reducing fuel consumption and emissions by minimizing unnecessary detours and delays. This aligns with broader goals of sustainable aviation and environmental responsibility, further emphasizing its significance in modern ATM and operational planning.

Overall, the results confirm that the model performs reliably in alternative ATS routing scenarios, demonstrating its effectiveness in addressing complex route planning challenges.

Its ability to adapt to changes while maintaining route feasibility and efficiency makes it a powerful tool for applications requiring dynamic navigation and optimized pathfinding under varying constraints.

4. CONCLUSION

Beyond serving as a dynamic decision-support tool for identifying alternative ATS routes when aircraft must divert to an alternate destination, this framework can be effectively applied to a variety of operational scenarios, significantly enhancing ATM efficiency and resilience. One of its key applications is the development of contingency flight paths tailored to specific airspace regions prone to frequent disruptions due to adverse weather conditions, high traffic density, or unforeseen technical issues. By preemptively designing such backup routes, air navigation service providers (ANSPs) can ensure seamless operational continuity, minimizing delays and optimizing airspace utilization under challenging circumstances. Furthermore, this model can play a crucial role in enhancing trajectory-based operations (TBO) by accurately determining real-time flight paths during various phases of operation.

Importantly, the implementation of alternative routing solutions in this model does not require fundamental changes to existing airspace structures or control sectors. Instead, it strategically utilizes current navigation aids, waypoints, and predefined air traffic corridors, enabling a seamless integration within existing ATM frameworks. This minimizes the need for costly infrastructural overhauls while maximizing the effectiveness of available airspace resources. This approach enhances flexibility and responsiveness while preserving the integrity of established airspace management systems. By adopting this model, ATC can proactively implement strategic decongestion measures, mitigating bottlenecks and optimizing sector workload distribution while adhering to established ATFM protocols. Moreover, the model enhances the capacity to provide real-time guidance in response to unforeseen situations, ensuring operational resilience. This adaptability is particularly valuable in high-density airspace, where the ability to swiftly reassign flight paths contributes to both safety and efficiency.

One significant advantage of this model is its adaptability to various airspace structures, achieved simply by modifying the input data, which consists of a list of waypoint coordinates and airports within the designated airspace. This flexibility allows for seamless integration into different ATM systems, optimizing navigation efficiency across diverse operational environments. This capability of the model ensures its applicability across a wide range of scenarios, from managing low-density regional airspaces to handling high-traffic international corridors. By dynamically adjusting to varying airspace configurations, the model enhances route planning, minimizes congestion, and contributes to the overall safety and efficiency of ATM.

Ultimately, this approach significantly strengthens flight safety, enhances operational predictability, and improves the adaptability of ATM systems without necessitating structural changes to the FIR. By integrating such a framework, ANSPs can modernize ATM operations, improve airspace utilization, and better align with next-generation aviation initiatives. By leveraging these advancements, the aviation industry can move toward a more intelligent ATM model that ensures greater flexibility, dynamism, and adaptability in all operational scenarios. This transformation is particularly crucial in an era of increasing air traffic demand, evolving regulatory frameworks, and the integration of emerging technologies such as artificial intelligence, automation, and unmanned aerial systems.

References

1. 6Wresearch. 2024. "Vietnam aviation market (2023-2029) outlook". Available at: https://www.6wresearch.com/industry-report/vietnam-aviation-market-outlook.
2. Beeker E. 2004. "Potential error in the reuse of Nilsson's A algorithm for path-finding in military simulations". *Journal of Defense Modeling and Simulation* 1(2). DOI: https://doi.org/10.1177/875647930400100203.
3. Bongo M.F., C.L. Sy. 2020. "A robust optimisation formulation for post-departure rerouting problem". In: *Proceedings of the IEEE International Conference on Industrial Engineering and Engineering Management*: 509-513. DOI: https://doi.org/10.1109/IEEM45057.2020.9309827.
4. Bureau of Transportation Statistics. 2025. "On-time performance – Reporting operating carrier flight delays at a glance". Available at: https://www.transtats.bts.gov/homedrillchart.asp.
5. Carreras R., C. Greenman. 2025. "Vietnam's vision of growth in the aeronautical industry". Available at: https://commons.erau.edu/publication/740.
6. Eurocontrol. 2024. "Cost of diversion". Available at: https://ansperformance.eu/economics/cba/standard-inputs/chapters/cost_of_diversion.html#eurocontrol-recommended-values.
7. Federal Aviation Administration. 2025. "Airport benefit-cost analysis guidance". Available at: https://www.faa.gov/sites/faa.gov/files/regulations_policies/policy_guidance/benefit_cost/FAA_Airport_Benefits_Guidance.pdf.
8. Felix Y.W., H.L.H.S. Warnars, L.L.H.S. Warnars, A. Ramadhan, T. Siswanto. 2024. "Searching routing using A-Star (A*) search algorithm". In: *Proceedings of the 3rd International Conference on Creative Communication and Innovative Technology (ICCIT)*: 1-7. DOI: https://doi.org/10.1109/ICCIT62134.2024.10701177.
9. Foead D., A. Ghifari, B.M. Kusuma, N. Hanafiah, E. Gunawan. 2021. "A systematic literature review of A* pathfinding". *Procedia Computer Science* 179: 507-514. DOI: https://doi.org/10.1016/j.procs.2021.01.034.
10. International Trade Administration. 2024. "Aviation: Country commercial guide – Vietnam". Available at: https://www.trade.gov/country-commercial-guides/vietnam-aviation.
11. Ji Y., X. Wu, Y. Shang, H. Fu, J. Yang, W. Wu. 2024. "Unmanned ground vehicle in unstructured environments applying improved A-star algorithm". In: *Proceedings of the 4th International Conference on Computer, Control and Robotics (ICCCR)*: 166-170. DOI: https://doi.org/10.1109/ICCCR61138.2024.10585482.
12. Ju C., Q. Luo, X. Yan. 2020. "Path planning using an improved A-star algorithm". In: *Proceedings of the 11th International Conference on Prognostics and System Health Management (PHM)*: 23-26. DOI: https://doi.org/10.1109/PHM-Jinan48558.2020.00012.
13. Kabir R., Y. Watanobe, M.R. Islam, K. Naruse. 2024. "Enhanced robot motion block of A-star algorithm for robotic path planning". *Sensors* 24(5): 1422. ISSN: 1424-8220. DOI: https://doi.org/10.3390/s24051422.
14. Kurniawan R., A. Armansyah, M. Idris. 2024. "Application of artificial intelligence in the design of 2D Escape From Pirates game with A Star algorithm search method". *Jurnal Dinda: Data Science, Information Technology, and Data Analysis* 4(2). DOI: https://doi.org/10.20895/dinda.v4i2.1558.

15. Li J., C. Yu, Z. Zhang, Z. Sheng, Z. Yan, X. Wu, W. Zhou, Y. Xie, J. Huang. 2023. "Improved A-star path planning algorithm in obstacle avoidance for the fixed-wing aircraft". *Electronics* 12(24): 5047. ISSN: 2079-9292. DOI: https://doi.org/10.3390/electronics12245047.
16. Ma L., H. Zhang, S. Meng, J. Liu. 2022. "Volcanic ash region path planning based on improved A-star algorithm". *Journal of Advanced Transportation*. DOI: https://doi.org/10.1155/2022/9938975.
17. Mandloi D., R. Arya, A.K. Verma. 2021. "Unmanned aerial vehicle path planning based on A* algorithm and its variants in 3D environment". *International Journal of System Assurance Engineering and Management* 12: 990-1000. DOI: https://doi.org/10.1007/s13198-021-01186-9.
18. Neretin E.S., A.S. Budkov, A.S. Ivanov. 2021. "Optimal four-dimensional route searching methodology for civil aircrafts". In: Li B., C. Li, M. Yang, Z. Yan, J. Zheng (Eds.). *IoT as a Service* 346: 433-442. Springer. DOI: https://doi.org/10.1007/978-3-030-67514-1_37.
19. Nguyen Ngoc Hoang Quan, V.N. Nechaev, V.B. Malygin. 2025. "Mathematical model and application of the A-star algorithm to optimize ATS routes in the Area Control Center Ho Chi Minh airspace". *Crede Experto: Transport, Society, Education, Language* 1: 64-78. ISSN: 2312-1327. DOI: https://doi.org/10.51955/2312-1327_2025_1_64.
20. OAG Aviation Worldwide Limited. 2024. "The busiest flight routes of 2024". Available at: https://www.oag.com/busiest-routes-world-2024.
21. Roy K.R. 2023. "Obstacle avoidance for quadcopters in formation flying based on A* algorithm". In: Jain K., V. Mishra, B. Pradhan (Eds.). *UASG 2021: Wings 4 Sustainability* 304: 443-456. Springer. DOI: https://doi.org/10.1007/978-3-031-19309-5_34.
22. Sathvik N.G., S. Patil. 2021. "Performance analysis of Dijkstra's and the A-star algorithm on an obstacle map". In: Bhateja V., S.C. Satapathy, C.M. Travieso-González, V.N.M. Aradhya (Eds.). *Data Engineering and Intelligent Computing* 1407: 81-90. Springer. DOI: https://doi.org/10.1007/978-981-16-0171-2_8.
23. VietnamPlus. 2025. "Flights diverted, delayed due to bad weather at Tan Son Nhat airport". Available at: https://en.vietnamplus.vn/flights-diverted-delayed-due-to-bad-weather-at-tan-son-nhat-airport-post253559.vnp.
24. Wang Y., L. Qian, M. Hong, Y. Luo, D. Li. 2024. "Multi-objective route planning model for ocean-going ships based on bidirectional A-star algorithm considering meteorological risk and IMO guidelines". *Applied Sciences* 14(17): 8029. ISSN: 2076-3417. DOI: https://doi.org/10.3390/app14178029.
25. Xu Y., R. Dalmau, M. Melgosa, A. Montlaur, X. Prats. 2020. "A framework for collaborative air traffic flow management minimizing costs for airspace users: Enabling trajectory options and flexible pre-tactical delay management". *Transportation Research Part B: Methodological* 134: 229-255. DOI: https://doi.org/10.1016/j.trb.2020.02.012.
26. Yang S., n Y. Ya, P. Chen. 2021. "Robust optimization models for flight rerouting". *International Journal of Computational Methods* 18(5). DOI: https://doi.org/10.1142/S0219876220400010.

Received 25.07.2025; accepted in revised form 30.10.2025